

## **Title: Proteomic profiling of the local and systemic immune response to pediatric respiratory viral infections**

### **Authors:**

Emily Lydon<sup>\*1</sup>, Christina M. Osborne<sup>\*2,3</sup>, Brandie D. Wagner<sup>4</sup>, Lilliam Ambroggio<sup>5,6</sup>, J. Kirk Harris<sup>6</sup>, Ron Reeder<sup>7</sup>, Todd C. Carpenter<sup>6</sup>, Aline B. Maddux<sup>6</sup>, Matthew K. Leroue<sup>6</sup>, Nadir Yehya<sup>2</sup>, Joseph L. DeRisi<sup>8,9</sup>, Mark W. Hall<sup>10</sup>, Athena F. Zuppa<sup>2</sup>, Joseph Carcillo<sup>11</sup>, Kathleen Meert<sup>12</sup>, Anil Sapru<sup>13</sup>, Murray M. Pollack<sup>14</sup>, Patrick McQuillen<sup>15</sup>, Daniel A. Notterman<sup>16</sup>, Charles R. Langelier<sup>+1,8</sup>, Peter M. Mourani<sup>+17</sup> for the Eunice Kennedy Shriver National Institute of Child Health and Human Development Collaborative Pediatric Critical Care Research Network (CPCCRN)

<sup>1</sup>Department of Medicine, University of California San Francisco, San Francisco, CA.

<sup>2</sup>Department of Anesthesiology and Critical Care Medicine, Children's Hospital of Philadelphia, Philadelphia, PA.

<sup>3</sup>Department of Pediatrics, Children's Hospital of Philadelphia, Philadelphia, PA.

<sup>4</sup>Department of Biostatistics and Informatics, University of Colorado, Colorado School of Public Health, Aurora, CO.

<sup>5</sup>Sections of Emergency Medicine and Hospital Medicine, Children's Hospital Colorado, Aurora, CO.

<sup>6</sup>Department of Pediatrics, University of Colorado School of Medicine and Children's Hospital Colorado, Aurora, CO.

<sup>7</sup>Department of Pediatrics, University of Utah, Salt Lake City, UT.

<sup>8</sup>Chan Zuckerberg Biohub, San Francisco, CA.

<sup>9</sup>Department of Biochemistry and Biophysics, University of California San Francisco, San Francisco, CA.

<sup>10</sup>Department of Pediatrics, Nationwide Children's Hospital, Columbus, OH.

<sup>11</sup>Departments of Pediatrics and Critical Care Medicine, University of Pittsburgh, Pittsburgh, PA.

<sup>12</sup>Department of Pediatrics, Children's Hospital of Michigan, Central Michigan University, Detroit, MI.

<sup>13</sup>Department of Pediatrics, University of California Los Angeles, Los Angeles, CA.

<sup>14</sup>Department of Pediatrics, Children's National Medical Center and George Washington School of Medicine and Health Sciences, Washington, DC.

<sup>15</sup>Department of Pediatrics, University of California San Francisco, San Francisco, CA.

<sup>16</sup>Department of Molecular Biology, Princeton University, Princeton, NJ.

<sup>17</sup>Department of Pediatrics, Critical Care, University of Arkansas for Medical Sciences and Arkansas Children's Hospital, Little Rock, AR.

\*Indicates equal contributions; +Indicates co-senior author.

### **Corresponding author:**

Charles Langelier, MD, PhD  
513 Parnassus Avenue, Room HSE401  
San Francisco, CA 94143  
Email: [chaz.langelier@ucsf.edu](mailto:chaz.langelier@ucsf.edu)

**Word count:** 2997

## ABSTRACT

Viral lower respiratory tract infection (vLRTI) is a leading cause of hospitalization and death in children worldwide. Despite this, no studies have employed proteomics to characterize host immune responses to severe pediatric vLRTI in both the lower airway and systemic circulation. To address this gap, gain insights into vLRTI pathophysiology, and test a novel diagnostic approach, we assayed 1,305 proteins in tracheal aspirate (TA) and plasma from 62 critically ill children using SomaScan. We performed differential expression (DE) and pathway analyses comparing vLRTI (n=40) to controls with non-infectious acute respiratory failure (n=22), developed a diagnostic classifier using LASSO regression, and analyzed matched TA and plasma samples. We further investigated the impact of viral load and bacterial coinfection on the proteome. The TA signature of vLRTI was characterized by 200 DE proteins ( $P_{adj} < 0.05$ ) with upregulation of interferons and T cell responses and downregulation of inflammation-modulating proteins including FABP and MIP-5. A nine-protein TA classifier achieved an AUC of 0.96 (95% CI 0.90-1.00) for identifying vLRTI. In plasma, the host response to vLRTI was more muted with 56 DE proteins. Correlation between TA and plasma was limited, although ISG15 was elevated in both compartments. In bacterial coinfection, we observed increases in the TNF-stimulated protein TSG-6, as well as CRP, and interferon-related proteins. Viral load correlated positively with interferon signaling and negatively with neutrophil-activation pathways. Taken together, our study provides fresh insight into the lower airway and systemic proteome of severe pediatric vLRTI, and identifies novel protein biomarkers with diagnostic potential.

## **IMPORTANCE**

We describe the first proteomic profiling of the lower airway and blood in critically ill children with severe viral lower respiratory tract infection (vLRTI). From tracheal aspirate (TA), we defined a proteomic signature of vLRTI characterized by increased expression of interferon signaling proteins and decreased expression of proteins involved in immune modulation including FABP and MIP-5. Using machine learning, we developed a parsimonious diagnostic classifier that distinguished vLRTI from non-infectious respiratory failure with high accuracy. Comparative analysis of paired TA and plasma specimens demonstrated limited concordance, although the interferon-stimulated protein ISG15 was significantly upregulated with vLRTI in both compartments. We further identified TSG-6 and CRP as airway biomarkers of bacterial-viral coinfection, and viral load analyses demonstrated positive correlation with interferon-related protein expression and negative correlation with the expression of neutrophil activation proteins. Taken together, our study provides new insight into the lower airway and systemic proteome of severe pediatric vLRTI.

## 1 INTRODUCTION

2 Respiratory viral infections are the most common cause of pediatric illness worldwide.<sup>1</sup> While  
3 often mild and self-limited, a substantial number of children progress to severe viral lower  
4 respiratory tract infection (vLRTI) requiring hospital admission and mechanical ventilation (MV),  
5 often further complicated by acute respiratory distress syndrome (ARDS) and/or bacterial  
6 coinfections. In a global epidemiological study of children under five, severe LRTI was the leading  
7 cause of mortality outside of the neonatal period, contributing to an estimated 760,000 deaths.<sup>2</sup>

8  
9 The marked heterogeneity in vLRTI clinical outcomes, driven in large part by differential host  
10 responses, remains poorly understood.<sup>3</sup> Deeply profiling the host immune response to vLRTI can  
11 offer insights into pathophysiology and also enable novel diagnostic test development.<sup>4,5</sup> Prior  
12 work evaluating the host response in LRTI using systems biology approaches has mainly focused  
13 on adult populations, and the few pediatric LRTI studies predominantly utilized transcriptomic or  
14 metabolomic approaches.<sup>6-10</sup> Proteomics, or the large-scale study of the protein composition  
15 within a biologic sample, has the potential to complement studies of the transcriptome, as protein  
16 expression is influenced by post-transcriptional regulation and may be a more direct reflection of  
17 cellular and immunologic processes.<sup>11</sup> The limited number of proteomic pediatric LRTI studies  
18 published to date have profiled plasma or urine samples,<sup>12-14</sup> which provide useful insights into  
19 the systemic response to LRTI and offer candidate diagnostic biomarkers, but may not reflect  
20 biological processes at the site of active infection. The local host proteomic response to severe  
21 viral infection in the lower respiratory tract remains poorly understood in children, as does the  
22 compartmentalization of proteomic responses in the blood versus airway.

23  
24 To address these questions, we perform high-dimensional proteomic profiling of paired tracheal  
25 aspirate (TA) and plasma samples in a prospective multicenter cohort of critically ill children with  
26 acute respiratory failure, specifically comparing vLRTI to non-infectious etiologies. We

27 hypothesized that there would be a distinct proteomic signature of vLRTI, more pronounced in the  
28 airway than blood, and that exploring proteomic correlations with bacterial-viral coinfection and  
29 viral load would yield valuable biological insights.

30

## 31 **METHODS**

### 32 *Description of cohort*

33 Children in this study represent a subset of those enrolled in a previously described prospective  
34 cohort of 454 mechanically ventilated children admitted to eight pediatric intensive care units in  
35 the National Institute of Child Health and Human Development's (NICHD) Collaborative Pediatric  
36 Critical Care Research Network (CPCCRN) from February 2015 to December 2017.<sup>8,9</sup> See  
37 supplementary material for enrollment criteria. IRB approval was granted for TA sample collection  
38 prior to consent, as endotracheal suctioning is standard-of-care. Specimens of children for whom  
39 consent was not obtained were destroyed. The study was approved by University of Utah IRB  
40 #00088656.

41

### 42 *Sample collection and processing*

43 TA specimens collected within 24 hours of intubation were processed for proteomic analysis, with  
44 centrifugation at 4°C at 15,000xg for five minutes and freezing of supernatant at -80°C in a  
45 microvial within 30 minutes. Some patients did not have TA samples available for proteomic  
46 analysis due to inadequate processing. Plasma samples collected within 24 hours of MV were  
47 frozen at -80°C. Some patients did not have plasma collected because consent was not obtained  
48 within the timeframe.

49

### 50 *Adjudication of LRTI status*

51 Adjudication was carried out retrospectively by study-site physicians who reviewed all clinical,  
52 laboratory, and imaging data following hospital discharge, with specific criteria detailed in the

53 supplementary material. Standard of care microbiological testing, including multiplex respiratory  
54 pathogen polymerase chain reaction (PCR) and semiquantitative bacterial respiratory cultures,  
55 were considered in the adjudication process. In addition, microbes detected by TA metagenomic  
56 next-generation sequencing (mNGS), as previously described,<sup>8</sup> were considered for pathogen  
57 identification. Patients were assigned a diagnosis of "vLRTI" if clinicians made a diagnosis of LRTI  
58 and the patient had a respiratory virus detected by PCR and/or mNGS. Within the vLRTI group,  
59 subjects were subcategorized as viral infection alone or bacterial coinfection, based on whether  
60 a bacterial respiratory pathogen was detected by bacterial culture, PCR, and/or mNGS. Patients  
61 alternatively were assigned a diagnosis of "No LRTI" if clinicians identified a clear, non-infectious  
62 cause of respiratory failure without clinical or microbiologic evidence of bacterial or viral LRTI.

63

#### 64 *Subject selection for proteomic analysis*

65 Subjects that were clinically adjudicated as vLRTI and No LRTI were selected for proteomics  
66 analysis, in an approximately 2:1 ratio. This subset of subjects represented a convenience sample  
67 of the larger cohort, with the goal of maximizing the number of subjects with both TA and plasma  
68 samples to allow comparative proteomic analysis, although not all subjects had all both samples  
69 available.

70

#### 71 *Proteomic analysis*

72 The SomaScan<sup>®</sup> 1.3k assay (SomaLogic) was utilized to quantify the protein expression in plasma  
73 and TA samples. The assay, described and validated elsewhere,<sup>15-17</sup> utilizes 1,305 single-  
74 stranded DNA aptamers that bind specific proteins, which are quantified on a customized Agilent  
75 hybridization assay. Aptamer measurement is therefore a surrogate of protein expression. The  
76 assay outputs fluorescence units that are relative but quantitatively proportional to the protein  
77 concentration in the sample.

78

79 *Statistical analysis*

80 Relative fluorescence units (RFUs) for each of the 1,305 protein aptamers were log-transformed  
81 for analysis. Differential expression was calculated between groups for each aptamer using limma,  
82 a R package that facilitates simultaneous comparisons between numerous targets.<sup>18</sup> Age-  
83 adjusted and age-unadjusted differential protein analyses were performed. Biological pathways  
84 were interrogated against the Reactome database with the R package WebGestaltR using a  
85 functional class scoring approach.<sup>19,20</sup> Specifically, the input list included the full set of 1,305  
86 proteins and the corresponding log<sub>2</sub>-fold change between the conditions of interest, ranked by T-  
87 statistic. P-values for protein and pathway analyses were adjusted for multiple comparisons using  
88 the Benjamini-Hochberg procedure; adjusted p-value ( $p_{adj}$ ) < 0.05 was considered statistically  
89 significant.

90

91 A parsimonious proteomic classifier was generated using LASSO logistic regression on TA  
92 samples with the cv.glmnet function in R, setting family = "binomial" and leaving other parameters  
93 as default.<sup>21</sup> LASSO was used for both feature selection and classification. The model was  
94 generated using five-fold cross-validation, where a model was trained on ~80% of samples and  
95 tested on ~20% of samples to generate vLRTI probabilities for each of the subjects in the cohort.  
96 To keep the fold composition comparable, we required at least 3 No LRTI subjects in each fold.  
97 AUC was calculated using the pROC package and confidence intervals were generated with  
98 bootstrapping.<sup>19</sup>

99

100 Correlation for each protein between TA and plasma samples were calculated using Pearson  
101 correlation, for all paired samples in bulk and then subdivided by group (vLRTI vs No LRTI).  
102 Correlation coefficients were considered strong if the absolute value was >0.5, moderate if 0.3-  
103 0.5, and weak if 0-0.3. Correlation between specific proteins and viral load were calculated

104 similarly. Viral load was extrapolated from mNGS reads-per-million, and if multiple viruses were  
105 detected, the viral loads were summed.

106

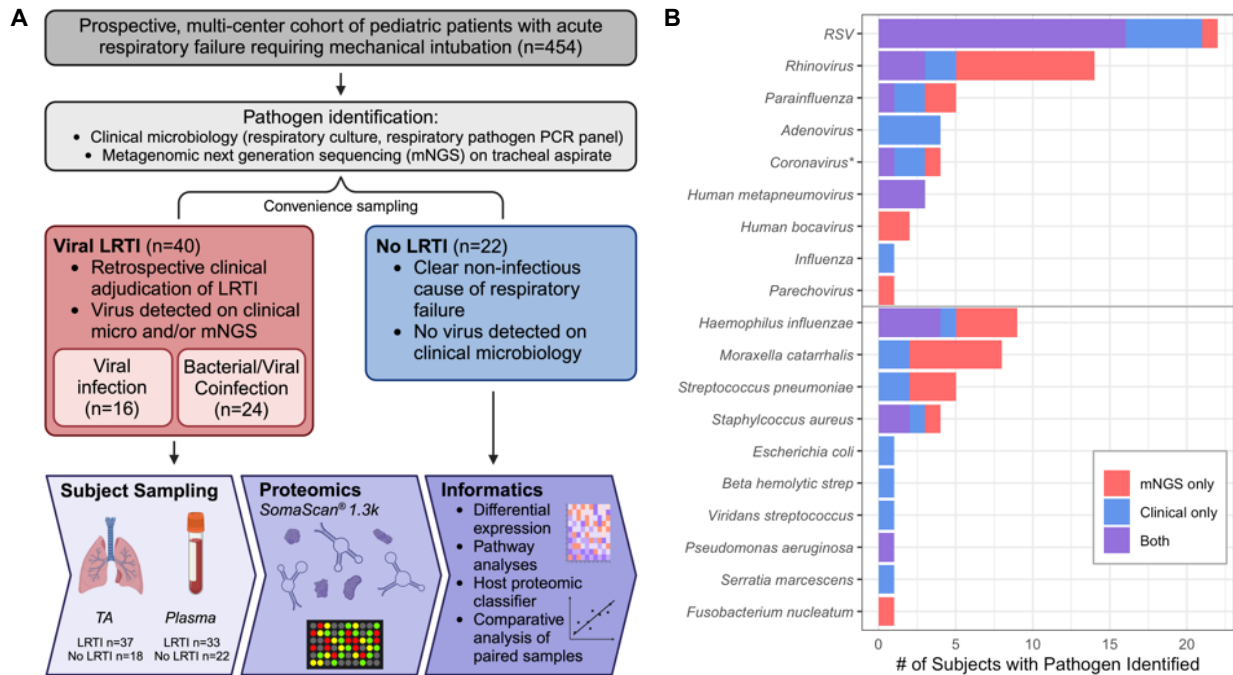
## 107 **RESULTS**

### 108 *Cohort characteristics and microbiology*

109 From the prospective multi-center cohort (n=454), samples from 62 subjects underwent proteomic  
110 analysis, including 40 with vLRTI and 22 with No LRTI (**Figure 1A**). Those with vLRTI were further  
111 subdivided into viral infection alone (n=16) or viral-bacterial coinfection (n=24). The demographic  
112 characteristics did not differ between the vLRTI and No LRTI groups, with the exception of age,  
113 which was higher in No LRTI than vLRTI (median 10.2 years [IQR 1.1-14.9] vs 0.9 [0.3-1.6]) (**Table**  
114 **1**). Diagnoses in the No LRTI group included trauma, neurologic conditions, ingestion, and  
115 anatomic airway abnormalities, with many having abnormal chest radiographs and meeting ARDS  
116 criteria. Within the vLRTI group, respiratory syncytial virus (RSV) was the most common pathogen,  
117 and 15 subjects had more than one virus (**Figure 1B**). *Haemophilus influenzae*, *Moraxella*  
118 *catarrhalis*, and *Streptococcus pneumoniae* were most common coinfecting bacterial pathogens.  
119



120



121  
122

123 **Figure 1: Study overview.** A) From a prospectively enrolled multicenter cohort of pediatric patients  
124 presenting with acute respiratory failure requiring intubation, 62 were selected for proteomic analysis. The  
125 vLRTI group included a subset of subjects who had bacterial coinfection. Plasma and tracheal aspirate (TA)  
126 samples collected on enrollment underwent proteomic profiling on the SomaScan® platform. Some subjects  
127 did not have all samples available for analysis, so the numbers available for each sample type are shown.  
128 Informatics approaches included evaluation of differentially expressed proteins and pathways, development  
129 of a host proteomic classifier, and comparative analyses of paired samples. B) Microbiology of the vLRTI  
130 group. Bar plot color indicates whether the microbe was detected on clinical microbiology, tracheal aspirate  
131 metagenomic next-generation sequencing (mNGS), or both. Many subjects had co-detection of multiple  
132 pathogens; thus, the total number of pathogens exceeds the number of patients in the vLRTI cohort.  
133 \*Coronavirus includes only non-SARS-CoV-2 coronaviruses.

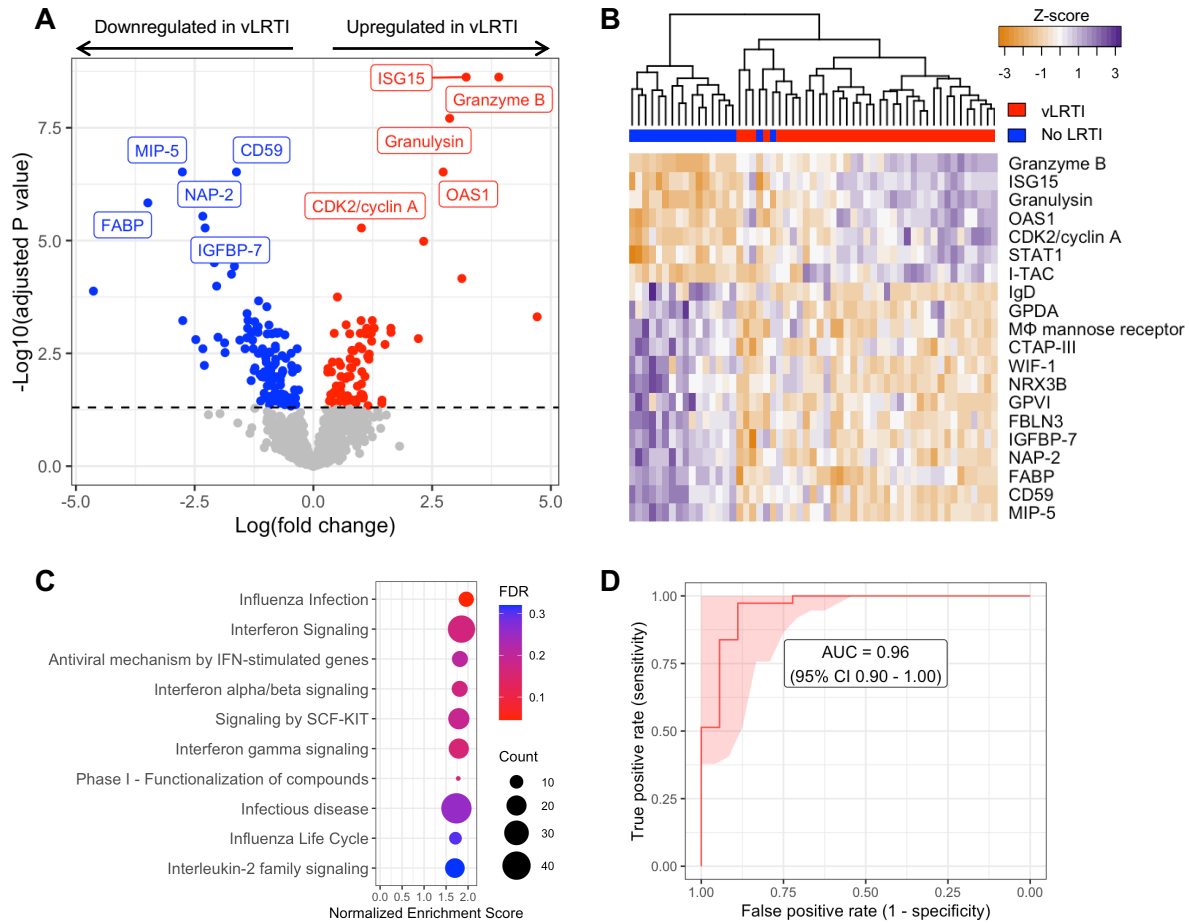
134 *Defining a lower respiratory tract proteomic signature of vLRTI*

135 We first compared protein expression in TA samples between the vLRTI (n=37) and No LRTI  
136 (n=18) groups. Two hundred proteins (15.3% of all proteins assayed) were differentially expressed  
137 at  $p_{\text{adj}} < 0.05$  (**Figure 2A, 2B**). Among the 80 proteins upregulated in vLRTI were interferon-  
138 stimulated ubiquitin-like protein ISG15 and oligoadenylate synthase protein OAS1, which are  
139 central to type I interferon signaling, and Granzyme B and Granulysin, proteins present in  
140 granules of cytotoxic T cells and natural killer (NK) cells. Among the 120 proteins downregulated  
141 in vLRTI were fatty acid-binding protein FABP, macrophage inhibitory protein MIP-5, and  
142 neutrophil-activating protein NAP-2. Pathway analysis confirmed interferon signaling as the  
143 primary pathway upregulated in the vLRTI group, although only the “influenza infection” pathway  
144 achieved  $p_{\text{adj}} < 0.05$  (**Figure 2C**).

145  
146 Having identified a strong host proteomic signature of vLRTI, we hypothesized that a  
147 parsimonious number of TA proteins could accurately differentiate vLRTI from No LRTI subjects.  
148 Utilizing LASSO logistic regression and employing five-fold cross-validation, we built  
149 parsimonious proteomic classifiers (ranging in size from 9 – 15 proteins) that accurately  
150 distinguished vLRTI and No LRTI with an area under the receiver operator curve (AUC) of 0.96  
151 (95% CI 0.90-1.00) (**Figure 2D, Table S1**). The proteins with consistently positive coefficients (i.e.  
152 increasing vLRTI probability) were Granulysin, Granzyme B, and ISG-15 as well as cyclin-  
153 dependent kinase protein CDK2 and kinesin-like protein KIF23. The proteins with consistently  
154 negative coefficients (i.e. decreasing probability of vLRTI) were FABP and NAP-2.

155  
156 Since age was statistically different between the two groups, we added age as a continuous  
157 covariate in our differential expression model (**Figure S1**). The results overall were similar, with  
158 176 differentially expressed proteins (58 upregulated and 118 downregulated with vLRTI). There

159 was considerable overlap (80%) in the top 10 most differentially expressed proteins between the  
 160 two models.  
 161



162  
 163  
 164 **Figure 2: Comparison of host protein expression between vLRTI and No LRTI cohorts in tracheal**  
 165 **aspirate.** A) Volcano plot of the differentially expressed proteins, with proteins significantly upregulated in  
 166 vLRTI in red, and proteins significantly downregulated in vLRTI in blue. The top ten proteins based on  $P_{\text{adj}}$   
 167 are labeled. B) Heat map showing differential expression of the top 20 proteins based on  $P_{\text{adj}}$  (rows) across  
 168 all patients (columns). Dendrogram clustering (top) highlights the proteomic differences between the two  
 169 groups. C) Pathway analysis showing the top ten pathways (all upregulated) ordered by Normalized  
 170 Enrichment Score. Dot color indicates the false discovery rate (FDR)  $P_{\text{adj}}$ , and size indicates the number of  
 171 proteins included in the pathway. D) Receiver operator characteristic (ROC) curve of the proteomic classifier  
 172 to distinguish vLRTI from No LRTI.

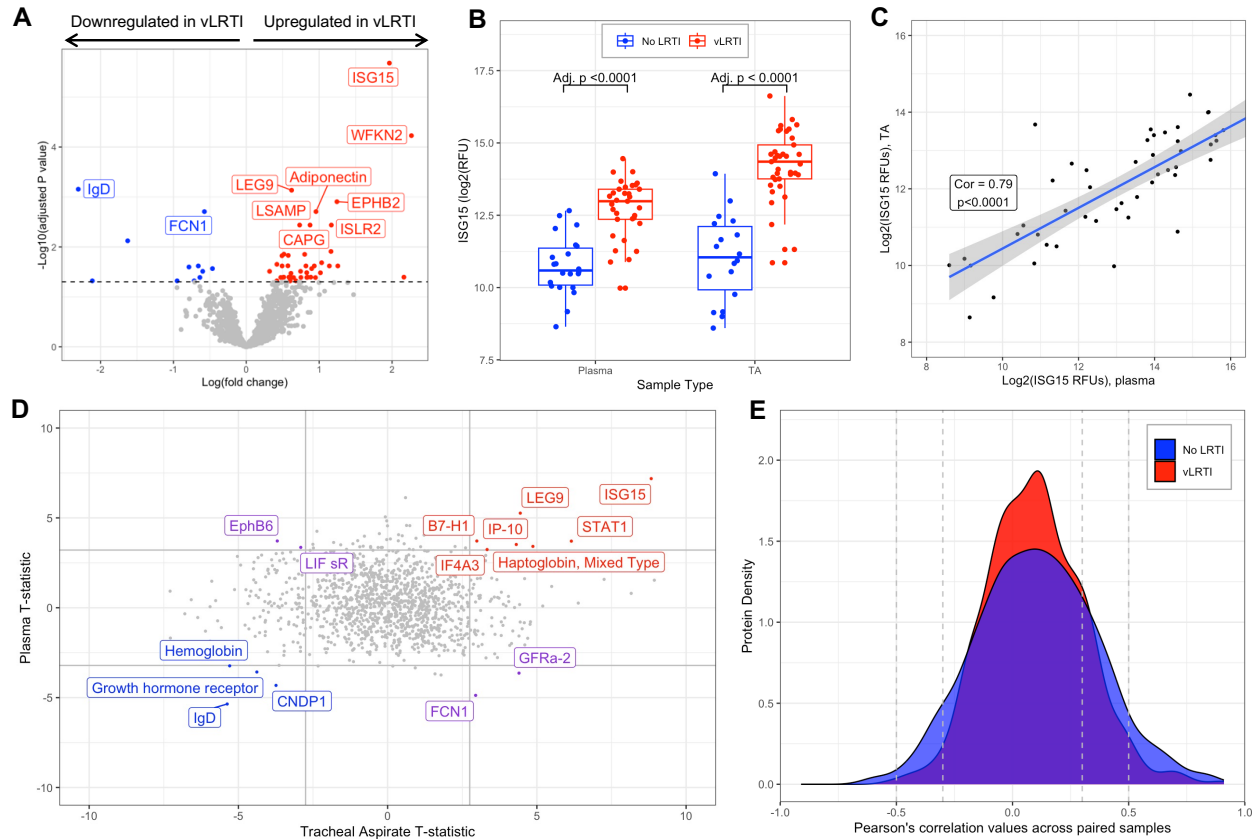
173 *Comparison of plasma proteomics between vLRTI and No LRTI groups*

174 We next compared plasma protein concentrations between vLRTI (n=33) and No LRTI (n=22)  
175 groups. The age-unadjusted differential expression analysis yielded 56 statistically significant  
176 proteins (4.3% of all proteins assayed), 45 upregulated in vLRTI and 11 downregulated in vLRTI  
177 (**Figure 3A**). However, adjusting for age, only one protein, ISG15, remained significant (**Figure**  
178 **S2**). ISG15, a type 1 interferon-stimulated protein, showed promise in distinguishing vLRTI and  
179 No LRTI groups in both plasma and TA ( $p_{\text{adj}}$  for both  $<0.0001$ ), and ISG15 expression was strongly  
180 correlated between paired TA and plasma samples (correlation coefficient 0.79,  $p<0.0001$ )  
181 (**Figure 3B, 3C**). ISG-15 alone implemented as a diagnostic test exhibited strong performance  
182 with AUCs of 0.95 (95% CI 0.89-1.00) and 0.91 (95% CI 0.83-0.99) in TA and plasma, respectively  
183 (**Figure S3**).

184

185 *Comparative analysis of plasma and respiratory tract proteomics*

186 Comparing the differentially expressed proteins between vLRTI and No LRTI groups in TA and  
187 plasma (using the age-unadjusted analyses), only 15 proteins were differentially expressed in  
188 both compartments, with seven proteins upregulated in vLRTI in both, four proteins  
189 downregulated in vLRTI in both, and four proteins with opposite directionality (**Figure 3D**). We  
190 further investigated protein correlation utilizing our paired samples (n=48 total paired TA and  
191 plasma samples from the same subject, including n=30 paired vLRTI samples and n=18 paired  
192 No LRTI samples). Correlation in expression between the lower airway and systemic circulation  
193 was weak for the majority of proteins (Pearson correlation coefficient -0.3 to +0.3) (**Figure 3E**),  
194 though there were exceptions, namely ISG-15.



195  
196  
197  
198  
199  
200  
201  
202  
203  
204  
205  
206

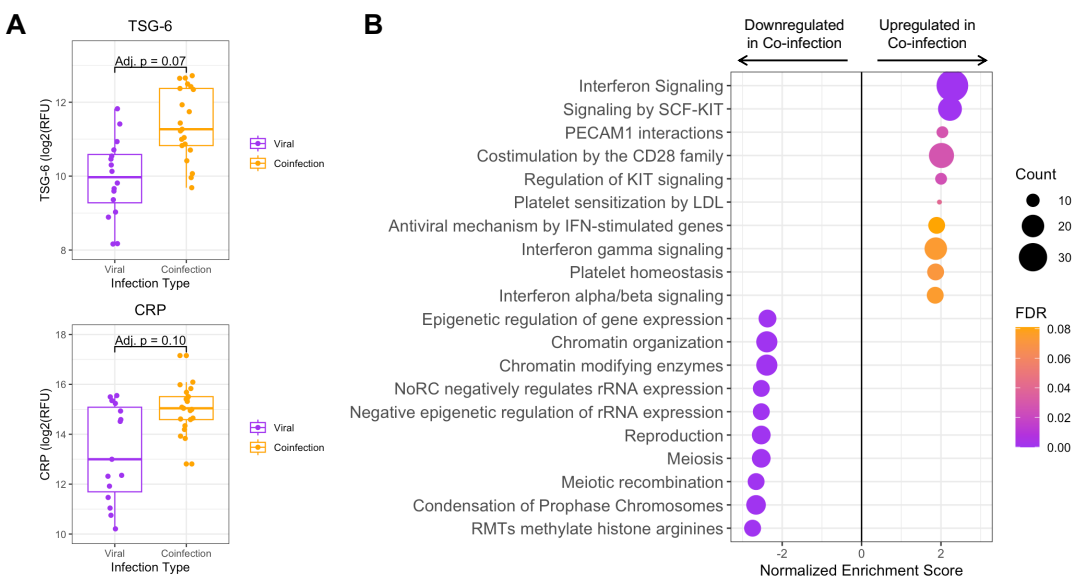
**Figure 3: Host protein expression in plasma and comparative proteomic analysis between plasma and tracheal aspirate samples.** A) Volcano plot of the differentially expressed plasma proteins in vLRTI versus No LRTI (age unadjusted). The top ten proteins based based on  $P_{adj}$  are labeled. B) Ubiquitin-like ISG-15 protein expression in plasma (left) and tracheal aspirate (TA) (right) in vLRTI (red) and No LRTI (blue) groups. C) Log-log plot showing correlation of ISG-15 values between paired plasma (x-axis) and TA (y-axis) samples. D) T statistics for each protein calculated with limma for vLRTI versus No LRTI comparisons in plasma and TA were plotted against one another. Proteins highlighted in red were significantly upregulated across both body compartments, in blue were downregulated in both, and in purple deviated in opposite directions. E) Density plot showing correlation coefficients for each protein in TA versus plasma, with stratification based on group (vLRTI in red vs No LRTI in blue).

207 *Lower respiratory tract proteomic differences in bacterial-viral coinfection*

208 Within the vLRTI group, subjects were categorized as either viral infection (n=16) or bacterial-viral  
209 coinfection (n=24) based on clinical microbiology and respiratory mNGS. Differential protein  
210 expression in TA between these two groups did not yield any statistically significant proteins at  
211  $p_{adj} < 0.05$ , but we did note an absolute increase in the expression of TSG-6, a tumor-necrosis  
212 factor-stimulated protein ( $p_{adj} = 0.07$ ) and C-reactive protein (CRP) ( $p_{adj} = 0.10$ ) in coinfection  
213 (**Figure 4A**). Pathway analysis showed heightened interferon signaling in coinfection compared

214 to viral infection alone. Pathways associated with cell turnover and division were preferentially  
 215 upregulated in viral infection compared to coinfection (**Figure 4B**).

216



217

218

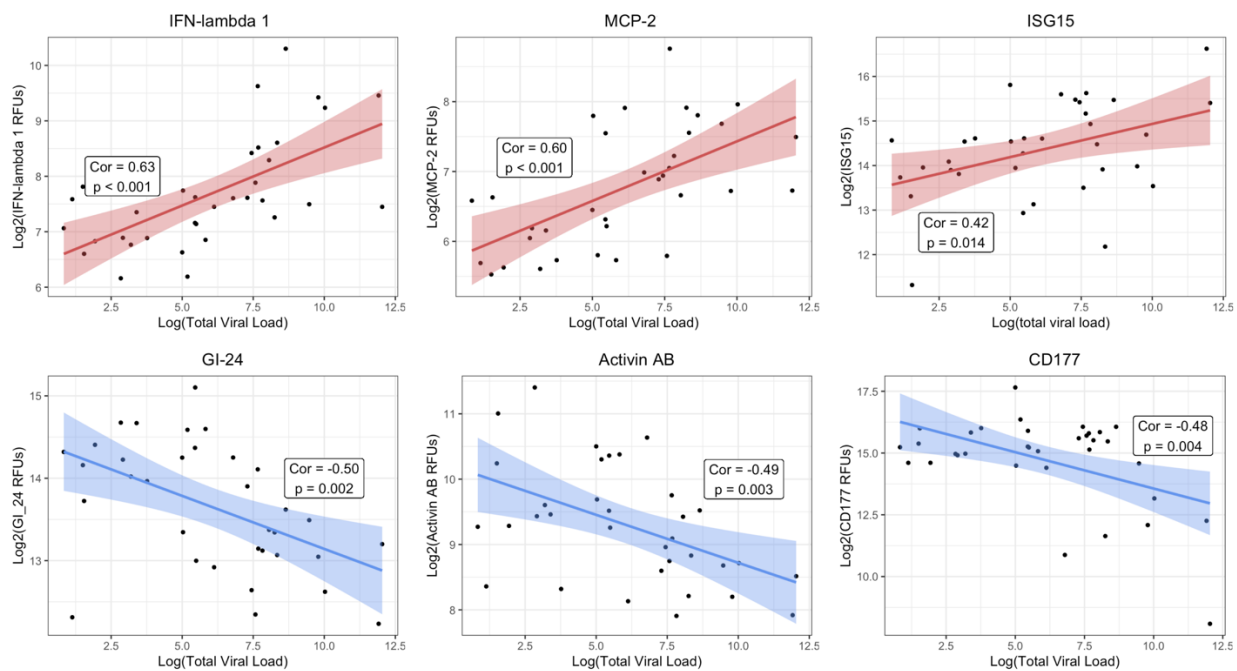
219 **Figure 4: Tracheal aspirate protein and pathway expression in bacterial-viral coinfection.**

220 A) Box plots of the two most differentially expressed proteins, tumor necrosis factor stimulated gene-6  
 221 (TSG-6) and C-reactive protein (CRP), between viral infection and coinfection subgroups. B) Pathway  
 222 analysis showing the top twenty pathways up- or down-regulated in bacterial-viral coinfection compared to  
 223 viral infection alone. Dot color indicates the false discovery rate (FDR)  $P_{adj}$ , and size indicates the number  
 224 of proteins included in the pathway.

225 *Lower respiratory tract protein correlations with viral load*

226 For the vLRTI subjects that tested positive for a virus by mNGS, the expression of TA proteins  
227 was correlated with viral load, measured as reads-per-million (**Figure 5**). Interferon-related  
228 proteins such as interferon-lambda 1 and ISG-15 were positively correlated with viral load, as well  
229 as monocyte chemotactic protein MCP-2. Conversely, platelet receptor GI-24, TFG- $\beta$  superfamily  
230 protein Activin AB, and neutrophil-activating glycoprotein CD177 were inversely correlated with  
231 viral load.

232



233

234

235 **Figure 5: Correlation of lower respiratory protein expression and viral load.** For each vLRTI subject  
236 with a virus detected on mNGS, correlation coefficients were calculated between viral load and relative  
237 concentration of each protein in TA. The top three highest positive correlations and the top three negative  
238 correlations are shown: interferon lambda-1 (IFN-lambda 1), monocyte chemotactic protein-2 (MCP-2);  
239 ubiquitin-like interferon stimulated gene-15 (ISG-15), platelet receptor GI-24, activin AB, and CD177.



240 **DISCUSSION**

241 In this study, we identified the proteomic signature of severe pediatric vLRTI in both the lower  
242 respiratory tract and systemic circulation, leveraging results to understand compartment-specific  
243 host responses, host-viral dynamics, and viral-bacterial coinfection, as well as identify specific  
244 proteins with diagnostic potential. This work represents the first simultaneous proteomic profiling  
245 of both TA and plasma samples from children with severe vLRTI.

246  
247 As hypothesized, the proteomic response to vLRTI was most robust at the local site of infection,  
248 with approximately 15% of assayed proteins differentially expressed in TA. This lower airway  
249 proteomic vLRTI signature was dominated by interferon-related proteins, which are well-known  
250 innate mediators of host defense and immunologic injury in viral infection.<sup>22</sup> In addition, this  
251 signature was enriched in proteins contained in cytotoxic lymphocytes that in turn secrete  
252 interferons.<sup>23</sup> Notable downregulated proteins were macrophage inhibitory protein-5 (MIP-5) and  
253 fatty acid binding protein (FABP), which has a diverse array of functions including macrophage  
254 regulation, suggesting that macrophage dynamics play an important role in response to vLRTI.<sup>24,25</sup>  
255 Interestingly, in the subanalysis of bacterial-viral coinfection, the expression of interferon-related  
256 proteins was even greater than in viral infection alone. Prior work, mostly in influenza infections,  
257 has suggested that type 1 interferons can suppress key neutrophil and macrophage defenses,  
258 increasing susceptibility to bacterial coinfection, which may explain this finding.<sup>26,27</sup>

259  
260 By integrating viral load measurements, we identified host TA proteins exhibiting proportional  
261 changes in expression based on viral load. Interferon-related proteins, including ISG-15 and  
262 interferon-lambda 1, and MCP-2, a chemokine induced by interferon signaling, exhibited the  
263 strongest induction in expression with viral load, underscoring the central role of interferons in  
264 innate antiviral defense. In contrast, the levels of CD177 (a glycoprotein involved in neutrophil  
265 activation),<sup>28</sup> Activin AB (a TGF- $\beta$  family protein implicated in ARDS inflammatory remodeling),<sup>29</sup>



266 and GI-24 (a platelet aggregation receptor)<sup>30</sup> all decreased in response to higher viral loads. As  
267 previously noted, impaired neutrophil responses have been implicated in the pathophysiology of  
268 post-viral bacterial pneumonia,<sup>26,27</sup> and our results suggest that this may occur in a viral-load  
269 dependent manner. Complementing these findings, a longitudinal transcriptomic study in adults  
270 hospitalized with severe influenza infection demonstrated initial upregulation of interferon  
271 pathways followed by inflammatory neutrophil activation and cell-stress patterns,<sup>31</sup> and a study of  
272 severe pediatric influenza infection found that early upregulation of genes associated with  
273 neutrophil degranulation were associated with multi-organ dysfunction and mortality.<sup>32</sup>

274

275 While we observed a robust protein signature of vLRTI in the lower airways, the findings in the  
276 peripheral blood were more subtle, and correlation between plasma and TA proteins was generally  
277 weak. Furthermore, we observed a greater impact of age on the blood proteomic signature of  
278 vLRTI, potentially because the signal in the peripheral blood was weaker and thus more  
279 susceptible to confounding. Understanding the systemic response to a local infection is certainly  
280 useful and practical, as peripheral blood samples and urine samples are less invasive to collect  
281 than lower respiratory samples and would allow for application in a broader population of children  
282 who do not require MV. However, to obtain the most informative and potent proteomic signal of  
283 infection, our findings suggest that sampling the site of infection has the highest yield. Supporting  
284 this intuitive finding is a comparative adult proteomic study assaying both serum and  
285 bronchoalveolar lavage in interstitial lung diseases which similarly found a much higher number  
286 of differentially expressed proteins in the lower respiratory tract compared to the blood.<sup>33</sup>

287

288 In addition to insights into the pathophysiology of vLRTI, our study also highlights the utility of  
289 proteomic approaches in diagnostic biomarker discovery. Standard-of-care multiplexed PCR  
290 assays only evaluate a limited subset of respiratory viruses<sup>34</sup> and cannot detect novel emerging  
291 viruses or differentiate asymptomatic carriage from true infection.<sup>35</sup> Host response-based assays

292 agnostic to viral species could be invaluable for pandemic preparedness and infection prevention  
293 in congregate settings. When employed as a diagnostic test to distinguish vLRTI from non-  
294 infectious respiratory failure, our nine-protein TA classifier achieved excellent performance with  
295 an AUC of 0.96. The single protein ISG15 also showed potential for use as a diagnostic biomarker  
296 in both TA and plasma. Type 1 interferons have previously been proposed as an accurate  
297 diagnostic screening test for pediatric viral infection.<sup>36</sup> Another diagnostic challenge in vLRTI is  
298 identifying bacterial coinfection, as standard respiratory bacterial cultures do not distinguish  
299 between coinfection and colonization and are often negative in the context of prior antibiotic  
300 administration. Our subanalysis of bacterial coinfection highlighted two TA proteins, TSG-6 (a  
301 tumor necrosis factor-inducible protein) and CRP (an inflammatory protein with modest specificity  
302 for bacterial LRTI in blood),<sup>37</sup> that may be useful respiratory biomarkers of secondary bacterial  
303 infection.

304

305 Our study has several strengths including our multi-center enrollment, clinical sampling at early  
306 time points, evaluation of protein expression in multiple compartments, and integration of  
307 respiratory mNGS for comprehensive pathogen evaluation. It also has several important  
308 limitations including small sample size which may have limited our ability to detect more subtle  
309 but clinically important differences in protein expression. Additionally, the version of the  
310 SomaScan<sup>®</sup> assay utilized does not encompass the entire human proteome, and we likely missed  
311 some important differentially expressed proteins and pathways. From the diagnostic biomarker  
312 standpoint, our findings are more preliminary in nature, and warrant further optimization and  
313 validation in larger cohorts with all relevant classes of infection (bacterial infection, viral infection,  
314 coinfection, and non-infectious controls) and a wider range of severity represented to rigorously  
315 understand performance. Finally, we recognize that there is no gold standard for LRTI diagnosis  
316 in children, and our reliance on the best practical methodology of combining retrospective clinical  
317 adjudication and microbiology results may have resulted in classification errors.

318

319 Taken together, we present a comprehensive proteomic characterization of severe pediatric vLRTI,  
320 highlighting pathophysiologic insights in both viral infection and bacterial-viral coinfection and  
321 deepening our understanding of compartmentalization of the human host response to LRTI.  
322 Validation of the present findings in larger external cohorts are needed with more in-depth analysis  
323 to determine whether new therapeutic targets can be identified and whether proteomic biomarkers  
324 may augment current standard-of-care pathogen-based diagnostic testing. Looking forward,  
325 multi-omic approaches combining proteomics and transcriptomics as well as integration with  
326 microbiology hold promise for advancing understanding of the heterogeneity of pediatric LRTI,  
327 modernizing diagnostics, and personalizing treatment.

328

#### 329 **FUNDING**

330 Support was provided by the Eunice Kennedy Shriver National Institute of Child Health and  
331 Human Development, the National Heart, Lung, and Blood Institute: UG1HD083171 and  
332 1R01HL124103 (Dr. Mourani), UG1HD049983 (Dr. Carcillo), UG1HD083170 (Dr. Hall),  
333 UG1HD050096 (Dr. Meert), UG1HD63108 (Dr. Zuppa), UG1HD083116 (Dr. Sapru),  
334 UG1HD083166 (Dr. McQuillen), UG1HD049981 (Dr. Pollack), K23HL138461 and 5R01HL155418  
335 (Dr. Langelier). The study was also supported by funding from the Chan Zuckerberg Biohub. The  
336 study sponsors were not involved in study design; in the collection, analysis, and interpretation of  
337 data; in the writing of the report; and in the decision to submit the report for publication.

338

#### 339 **DECLARATION OF INTERESTS**

340 The authors declare no conflicts of interest.

341

342 **DATA AVAILABILITY**

343 Proteomic data, subject metadata, and code for reproducing the results of this study can be

344 found at: <https://github.com/infectiousdisease-langelier-lab/pedsLRTIproteomics>.

345 **TABLES**

346 **Table 1: Demographic and clinical characteristics of the vLRTI and No LRTI cohorts.**

	<b>vLRTI (n=40)</b>	<b>No LRTI (n=22)</b>	<b>P value*</b>
<b>Female, n (%)</b>	18 (45.0%)	11 (50.0%)	0.79
<b>Age in years, median (IQR)</b>	0.9 (0.3 - 1.6)	10.2 (1.1-14.9)	<0.01
<b>Race</b>			0.71
<b>White, n (%)</b>	26 (65.0%)	14 (63.6%)	
<b>Black/African American, n (%)</b>	6 (15.0%)	6 (27.3%)	
<b>Asian, n (%)</b>	1 (2.5%)	1 (4.5%)	
<b>Native Hawaiian/Pacific Islander, n (%)</b>	1 (2.5%)	0 (0.0%)	
<b>American Indian/Alaska Native, n (%)</b>	1 (2.5%)	0 (0.0%)	
<b>Unknown/Not Reported, n (%)</b>	5 (12.5%)	1 (4.5%)	
<b>Hispanic/Latino ethnicity, n (%)</b>	8 (20.0%)	1 (4.5%)	0.14
<b>Comorbidity, n (%)</b>	14 (35.0%)	11 (50.0%)	0.29
<b>Immunocompromise, n (%)</b>	1 (2.5%)	0 (0.0%)	0.99
<b>Admission category</b>			<0.01
<b>Medical, n (%)</b>	40 (100%)	14 (63.6%)	
<b>Surgical, n (%)</b>	0 (0.0%)	5 (22.7%)	
<b>Trauma, n (%)</b>	0 (0.0%)	3 (13.6%)	
<b>Infiltrates on initial CXR, n (%)</b>	36 (90.0%)	12 (54.5%)	<0.01
<b>ARDS, n (%)</b>	18 (45.0%)	4 (18.0%)	0.05
<b>Received antibiotics, n (%)</b>	14 (35.0%)	8 (36.4%)	0.99
<b>Ventilator days, median (IQR)</b>	6 (5.0-9.0)	6 (5.0-8.0)	0.85
<b>ICU length of stay in days, median (IQR)</b>	10 (8.0-16.5)	9 (6.3-13.3)	0.25
<b>Hospital length of stay in day, median (IQR)</b>	14 (10.5-19.5)	16 (9.5-38.8)	0.34
<b>Mortality, n (%)</b>	1 (2.5%)	3 (13.6%)	0.12

347 \*Wilcoxon rank sum test used for all continuous variables. Fisher's exact test used for all  
 348 categorical variables. IQR, interquartile range; ARDS, acute respiratory distress syndrome; ICU,  
 349 intensive care unit.

350 **REFERENCES**

- 351
- 352 1 Hemming VG. Viral respiratory diseases in children: Classification, etiology, epidemiology,  
353 and risk factors. *The Journal of Pediatrics* 1994; **124**: S13.
- 354 2 Liu L, Oza S, Hogan D, *et al.* Global, regional, and national causes of under-5 mortality in  
355 2000–15: an updated systematic analysis with implications for the Sustainable Development  
356 Goals. *Lancet* 2016; **388**: 3027–35.
- 357 3 Rouse BT, Sehrawat S. Immunity and immunopathology to viruses: what decides the  
358 outcome? *Nat Rev Immunol* 2010; **10**: 514–26.
- 359 4 Zaas AK, Garner BH, Tsalik EL, Burke T, Woods CW, Ginsburg GS. The current epidemiology  
360 and clinical decisions surrounding acute respiratory infections. *Trends Mol Med* 2014; **20**:  
361 579–88.
- 362 5 Troy NM, Bosco A. Respiratory viral infections and host responses; insights from genomics.  
363 *Respiratory Research* 2016; **17**: 156.
- 364 6 Wildman E, Mickiewicz B, Vogel HJ, Thompson GC. Metabolomics in pediatric lower  
365 respiratory tract infections and sepsis: a literature review. *Pediatr Res* 2023; **93**: 492–502.
- 366 7 Casini F, Valentino MS, Lorenzo MG, *et al.* Use of transcriptomics for diagnosis of infections  
367 and sepsis in children: A narrative review. *Acta Paediatrica* 2024; **113**: 670–6.
- 368 8 Mick E, Tsitsiklis A, Kamm J, *et al.* Integrated host/microbe metagenomics enables accurate  
369 lower respiratory tract infection diagnosis in critically ill children. *J Clin Invest* 2023; **133**.  
370 DOI:10.1172/JCI165904.
- 371 9 Mourani PM, Sontag MK, Williamson KM, *et al.* Temporal airway microbiome changes related  
372 to ventilator-associated pneumonia in children. *European Respiratory Journal* 2021; **57**.  
373 DOI:10.1183/13993003.01829-2020.
- 374 10 Dapat C, Kumaki S, Sakurai H, *et al.* Gene signature of children with severe respiratory  
375 syncytial virus infection. *Pediatr Res* 2021; **89**: 1664–72.
- 376 11 Pereira-Fantini PM, Tingay DG. The proteomics of lung injury in childhood: challenges and  
377 opportunities. *Clin Proteomics* 2016; **13**: 5.
- 378 12 Cheng J, Ji D, Yin Y, *et al.* Proteomic profiling of urinary small extracellular vesicles in  
379 children with pneumonia: a pilot study. *Pediatr Res* 2023; **94**: 161–71.
- 380 13 Tsai M-H, Lin T-Y, Hsieh S-Y, Chiu C-Y, Chiu C-H, Huang Y-C. Comparative proteomic studies  
381 of plasma from children with pneumococcal pneumonia. *Scandinavian Journal of Infectious  
382 Diseases* 2009; **41**: 416–24.
- 383 14 Yin G-Q, Zeng H-X, Li Z-L, *et al.* Differential proteomic analysis of children infected with  
384 respiratory syncytial virus. *Braz J Med Biol Res* 2021; **54**: e9850.
- 385 15 Gold L, Ayers D, Bertino J, *et al.* Aptamer-based multiplexed proteomic technology for  
386 biomarker discovery. *PLoS One* 2010; **5**: e15004.
- 387 16 Kim CH, Tworoger SS, Stampfer MJ, *et al.* Stability and reproducibility of proteomic profiles  
388 measured with an aptamer-based platform. *Sci Rep* 2018; **8**: 8382.
- 389 17 Candia J, Cheung F, Kotliarov Y, *et al.* Assessment of Variability in the SOMAscan Assay. *Sci  
390 Rep* 2017; **7**: 14248.
- 391 18 Ritchie ME, Phipson B, Wu D, *et al.* limma powers differential expression analyses for RNA-  
392 sequencing and microarray studies. *Nucleic Acids Res* 2015; **43**: e47.
- 393 19 Milacic M, Beavers D, Conley P, *et al.* The Reactome Pathway Knowledgebase 2024. *Nucleic  
394 Acids Research* 2024; **52**: D672–8.
- 395 20 Wang J, Vasaikar S, Shi Z, Greer M, Zhang B. WebGestalt 2017: a more comprehensive,  
396 powerful, flexible and interactive gene set enrichment analysis toolkit. *Nucleic Acids  
397 Research* 2017; **45**: W130–7.
- 398 21 Tay JK, Narasimhan B, Hastie T. Elastic Net Regularization Paths for All Generalized Linear  
399 Models. *Journal of Statistical Software* 2023; **106**: 1–31.

- 400 22Mesev EV, LeDesma RA, Ploss A. Decoding type I and III interferon signalling during viral  
401 infection. *Nat Microbiol* 2019; **4**: 914–24.
- 402 23de Jong LC, Crnko S, ten Broeke T, Bovenschen N. Noncytotoxic functions of killer cell  
403 granzymes in viral infections. *PLoS Pathog* 2021; **17**: e1009818.
- 404 24Jin R, Hao J, Yi Y, Sauter E, Li B. Regulation of macrophage functions by FABP-mediated  
405 inflammatory and metabolic pathways. *Biochim Biophys Acta Mol Cell Biol Lipids* 2021; **1866**:  
406 158964.
- 407 25Storch J, Thumser AE. Tissue-specific Functions in the Fatty Acid-binding Protein Family. *J*  
408 *Biol Chem* 2010; **285**: 32679–83.
- 409 26Connolly E, Hussell T. The Impact of Type 1 Interferons on Alveolar Macrophage Tolerance  
410 and Implications for Host Susceptibility to Secondary Bacterial Pneumonia. *Front Immunol*  
411 2020; **11**: 495.
- 412 27Mehta D, Petes C, Gee K, Basta S. The Role of Virus Infection in Deregulating the Cytokine  
413 Response to Secondary Bacterial Infection. *J Interferon Cytokine Res* 2015; **35**: 925–34.
- 414 28Bai M, Grieshaber-Bouyer R, Wang J, *et al.* CD177 modulates human neutrophil migration  
415 through activation-mediated integrin and chemoreceptor regulation. *Blood* 2017; **130**: 2092–  
416 100.
- 417 29de Kretser DM, Bensley JG, Pettilä V, *et al.* Serum activin A and B levels predict outcome in  
418 patients with acute respiratory failure: a prospective cohort study. *Crit Care* 2013; **17**: 1–13.
- 419 30Devanathan V, Hagedorn I, Köhler D, *et al.* Platelet G $\alpha$ i2 protein G $\alpha$ i2 is an essential mediator  
420 of thrombo-inflammatory organ damage in mice. *Proc Natl Acad Sci U S A* 2015; **112**: 6491–  
421 6.
- 422 31Dunning J, Blankley S, Hoang LT, *et al.* Progression of whole-blood transcriptional signatures  
423 from interferon-induced to neutrophil-associated patterns in severe influenza. *Nat Immunol*  
424 2018; **19**: 625–35.
- 425 32Novak T, Crawford JC, Hahn G, *et al.* Transcriptomic profiles of multiple organ dysfunction  
426 syndrome phenotypes in pediatric critical influenza. *Front Immunol* 2023; **14**: 1220028.
- 427 33Majewski S, Zhou X, Miłkowska-Dymanowska J, Białas AJ, Piotrowski WJ, Malinowski A.  
428 Proteomic profiling of peripheral blood and bronchoalveolar lavage fluid in interstitial lung  
429 diseases: an explorative study. *ERJ Open Research* 2021; **7**. DOI:10.1183/23120541.00489-  
430 2020.
- 431 34García-Arroyo L, Prim N, Martí N, Roig MC, Navarro F, Rabella N. Benefits and drawbacks of  
432 molecular techniques for diagnosis of viral respiratory infections. Experience with two  
433 multiplex PCR assays. *J Med Virol* 2016; **88**: 45–50.
- 434 35Jansen RR, Wieringa J, Koekkoek SM, *et al.* Frequent Detection of Respiratory Viruses  
435 without Symptoms: Toward Defining Clinically Relevant Cutoff Values  $\nabla$ . *J Clin Microbiol*  
436 2011; **49**: 2631–6.
- 437 36Trouillet-Assant S, Viel S, Ouziel A, *et al.* Type I Interferon in Children with Viral or Bacterial  
438 Infections. *Clinical Chemistry* 2020; **66**: 802–8.
- 439 37van der Meer V, Neven AK, van den Broek PJ, Assendelft WJJ. Diagnostic value of C  
440 reactive protein in infections of the lower respiratory tract: systematic review. *BMJ* 2005; **331**:  
441 26.  
442